

# Dielectric Ba(Ti<sub>1-x</sub>Sn<sub>x</sub>)O<sub>3</sub> ( $x = 0.13$ ) ceramics, sintered by spark plasma and conventional methods

Gheorghe Aldica · Marin Cernea · Paul Ganea

Received: 25 November 2009 / Accepted: 12 January 2010 / Published online: 26 January 2010  
© Springer Science+Business Media, LLC 2010

**Abstract** A two-step sintering approach composed of spark-plasma-sintering (SPS) technique at 1000 °C for 1 min and under a uniaxial pressure of 63 MPa followed by conventional sintering at 1400 °C for 3 h is proposed for synthesis of dense Ba(Ti<sub>0.87</sub>Sn<sub>0.13</sub>)O<sub>3</sub> ceramics. Starting powders had grain size of about 90 nm and were obtained by co-precipitation. The SPS pellets consist of submicron (300–500 nm) grains. X-ray diffraction analysis of as-prepared Ba(Ti<sub>0.87</sub>Sn<sub>0.13</sub>)O<sub>3</sub> ceramic shows the occurrence of cubic and tetragonal phase coexistence for the pellets obtained after SPS processing and the presence of only tetragonal phase in the samples after the second (conventional) sintering. Grain uniformity in the final product is high, with average size of ~2 μm. The apparent densities of the sintered pellets at temperature of 1400 °C were ~92% of the theoretical value of Ba(Ti<sub>0.87</sub>Sn<sub>0.13</sub>)O<sub>3</sub>. The ceramics exhibit a high relative dielectric constant of 6,550 and a dielectric loss ( $\tan \delta$ ) = 0.078 at Curie temperature of 63 °C and 10 Hz.

## Introduction

Solid solutions BaTi<sub>1-x</sub>Sn<sub>x</sub>O<sub>3</sub> (BTS<sub>x</sub>) show interesting dielectric properties and are used for capacitors, relaxors and sensor [1–4]. The isovalent substitution of Ti<sup>4+</sup> by Sn<sup>4+</sup> ions in barium titanate leads to a reduced stability range of the tetragonal phase, due to a decrease of the ferroelectric cubic-tetragonal phase transition temperature  $T_c$  [5–8]. Sn substitution gradually shifts the first order

character of the phase transition in BaTiO<sub>3</sub> towards a second order transition. The character of the ferroelectric phase transition in BTS<sub>x</sub> strongly depends on the Sn-level  $x$ . The observation of ferroelectric domains below the permittivity maximum temperature provided evidence of ferroelectric long-range order for  $x \leq 0.13$ , whereas indication for the relaxor state of BTS<sub>x</sub> was obtained for compositions  $x \geq 0.2$  [6, 9].

Both the variation of the chemical composition, reduction of grain size and reduction of grain boundaries improve the temperature stability of electric properties in ferroelectric ceramics. Use of fine powders as precursors in combination with SPS is thought to be convenient in order to have a better control of the indicated parameters [10]. Using SPS, it is possible to preserve and control the grain size and to some extent the grain boundaries. We note that SPS was used with good results for sintering of BaTiO<sub>3</sub> [11–13] ceramic starting from mixtures of oxides and carbonates.

Most data available for BTS<sub>x</sub> focus on ceramics sintered from conventional powders, obtained from solid state reaction of BaCO<sub>3</sub> with TiO<sub>2</sub>, SnO<sub>2</sub> or mixtures of both oxides. Few chemical techniques such as precipitation [14] and glycolate-precursor based synthesis [15] have been used to fabricate ultra-fine BTS<sub>x</sub> powders.

In this paper, preparation and dielectric characterization of BTS<sub>13</sub> ceramic, processed by spark plasma and conventional sintering from co-precipitated powders are reported.

## Experimental procedure

The BTS<sub>13</sub> powder obtained by co-precipitation [14] was sintered into discs with thickness of 1.5 mm and diameter

G. Aldica (✉) · M. Cernea · P. Ganea  
National Institute of Materials Physics, Str. Atomistilor 105 Bis,  
RO-77125, P.O. Box MG-7, Magurele, Bucharest, Romania  
e-mail: aldica@infim.ro

of 19 mm by SPS technique using SPS 825S (Sumitomo Coal Mining Co, Japan) equipment as follows:  $\text{BTS}_{13}$  powder was poured into the graphite die and then sintered at 1000 °C, for 1 min. A type K thermocouple measured the temperature. The hot junction of the thermocouple was placed into a horizontal channel at about 7 mm deep in the 12.7 mm thick die wall. The heating rate was chosen as 250 °C  $\text{min}^{-1}$  and the applied mechanical uniaxial pressure was 63 MPa. Sintering was performed in vacuum (6–15 Pa). In the SPS apparatus the default 12:2 (on:off) current pulsed pattern was applied. The waveform is not square and, in fact, is composed of several spikes (pulses) separated by a current-free interval. Regardless of the pattern, each pulse has the same period of about 3 ms. Thus, the pattern of 12:2 has a sequence of 12 pulses ‘on’ and 2 pulses with no current (off). The total time of one sequence (cycle) is about 0.04 s. The operating parameters, namely voltage and the peak current were below 5 V and 2000 A, respectively.

Figure 1 shows the variation of displacement,  $d$ , its rate,  $r$ , and operating current,  $I$ , as a function of temperature, during the SPS process of  $\text{BTS}_{13}$  powder. The displacement is measured between of two punches of die in the cylindrical configuration, where is pressed and compacted the  $\text{BTS}_{13}$  powder. Finally we get a dense and tick disc.

The onset temperature of the densification process is 885 °C and the offset temperature is placed above 950 °C, where the operating current decreased. X-ray diffraction indicated the presence of cubic and tetragonal  $\text{BTS}_{13}$  phases (see Fig. 4a in “X-ray patterns” section). To obtain a tetragonal single phase ceramic, a second step of conventional sintering on as-prepared SPS bulks was applied at 1400 °C for 3 h in air. But, before that, SPS-samples were annealed in oxygen, at 950 °C for 3 h to remove the carbon contamination from the graphite die and punches.

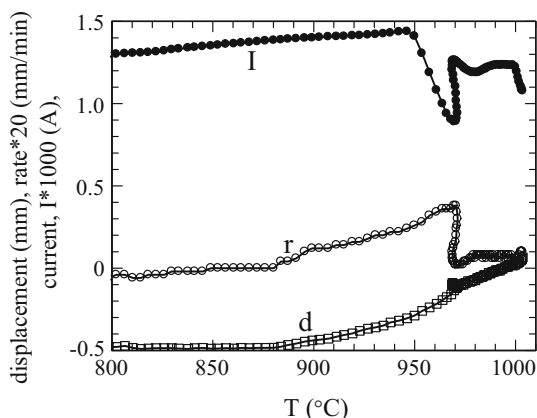


**Fig. 1** Displacement (shrinkage), its rate and operating current versus temperature for  $\text{BTS}_{13}$  sample

The microstructure of the samples was investigated using a Hitachi S2600N scanning electron microscope. The structure of the  $\text{BTS}_{13}$  precursor powders was characterized by X-ray diffraction technique using a Bruker-AXS tip D8 ADVANCE diffractometer. For powder diffraction,  $\text{CuK}_{\alpha 1}$  radiation, (wavelength 1.5406 Å), a LiF crystal monochromator and Bragg–Brentano diffraction geometry were used. The data were acquired at 25 °C with a step-scan interval of 0.020° and a step time of 10 s.

Apparent densities of the sintered pellets were measured by Archimedes method (in water) using a density balance.

The temperature dependence of dielectric constant and dielectric losses were evaluated in the temperature range from –20 to 120 °C at 10 Hz, 100 Hz, 1 kHz, 10 kHz and 100 kHz by an Agilent 4263B LCR meter equipped with a thermostat. The electrical measurements were carried out in the metal–ferroelectric–metal (MFM) configuration where M is silver and F is the ferroelectric sample ( $\text{BTS}_{13}$ ). Silver paste used as the electrodes, was screen-printed on both surfaces of  $\text{BTS}_{13}$  pellets.

## Results and discussion

### Microstructure

The SEM micrograph of  $\text{BTS}_{13}$  starting powders shows agglomerates consisting of homogenous-sized grains (~90 nm in diameter) (Fig. 2). The homogeneity of the grain size of the starting powders enhances the densification process [11] of  $\text{BaTiO}_3$ .

The densities of pellets sintered by SPS were about 83.5% of the theoretical density.

After SPS, the surface of the bulk  $\text{BTS}_{13}$  samples was contaminated with carbon from the graphite foils inserted

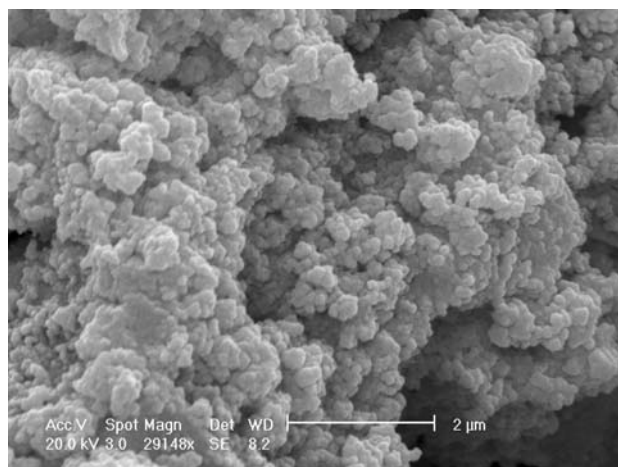


**Fig. 2** Scanning electron microscope photomicrographs of the  $\text{BTS}_{13}$  powder

between the die, punches and the ceramic powder. In the volume, these samples were dark blue due to the reducing sintering atmosphere used during SPS (low vacuum). In this way, some  $Ti^{4+}$  is reduced to  $Ti^{3+}$ , a well known phenomena in SPS sintering [11]. To restore the oxygen stoichiometry and to remove the carbon contamination, SPS dense pellets were annealed in oxygen, at 950 °C for 3 h. Corresponding typical SEM images of the fractured surface of the annealed pellets are shown in Fig. 3a. Similar SEM images were obtained by Takeuchi et al. [12] for  $BaTiO_3$  SPS pellets.

The SPS pellets consist of submicron (300–500 nm) grains (Fig. 3a). This result indicates, as expected, that the

short sintering period is an essential factor to obtain fine-grained  $BTS_{13}$  ceramics by the SPS process. Some pores located at grain boundaries can be observed. The grain size and shape was highly uniform for the prepared samples. The apparent density of the pellets sintered by SPS technique and annealed at 950 °C, 3 h in oxygen was about 86.5% of the theoretical value (taken 6.19 g/cm<sup>3</sup>, [16]) of  $BTS_{13}$ .

The sintering process started by SPS method was continued by the second step conventional sintering at 1400 °C for 3 h in air. The final ceramics show the grains with average size of  $\sim 2 \mu m$  (Fig. 3b). The apparent densities of the sintered pellets at temperature of 1400 °C were  $\sim 92\%$  of the theoretical value of  $BTS_{13}$ .

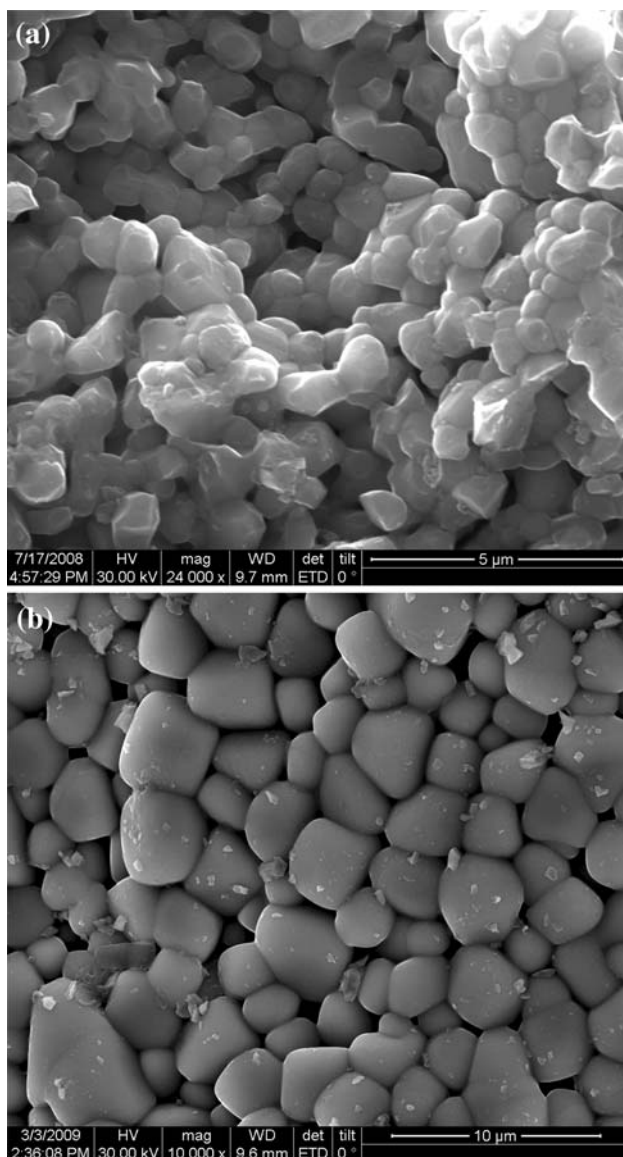


**Fig. 3** SEM images of fracture surface of the  $BTS_{13}$  pellets annealed at 950 °C, 3 h in oxygen (a), and the conventional sintering at 1400 °C, 3 h in air (b)

#### X-ray patterns

Figure 4a, b shows the XRD patterns of  $BTS_{13}$  pellets, annealed at 950 °C, 3 h in oxygen, after spark-plasma sintering and final sintering at 1400 °C for 3 h, respectively. Figure 4c presents a detailed look at the (200) peak for the sample after heating at 950 and 1400 °C. Figure 4a indicates that the crystalline structure of the decarbonised SPS pellets (at 950 °C) consists of cubic phase  $BaTiO_3$  (XRD pattern PDF 79-2263) [17] and to a small secondary phase  $Ti_3O_5$ , monoclinic (XRD pattern PDF 01-076-1066).

The diffraction patterns of  $BTS_{13}$  pellets sintered at 1400 °C shown that the peak  $2\theta = 45.4^\circ$  splits into (002) and (200) reflections (Fig. 4c), which are characteristic to  $BaTiO_3$  tetragonal phase (PDF 81-2202) [18]. Figure 4b indicates also a small secondary phase (orthorhombic  $Ba_2TiO_4$ ) (PDF 01-075-0677).

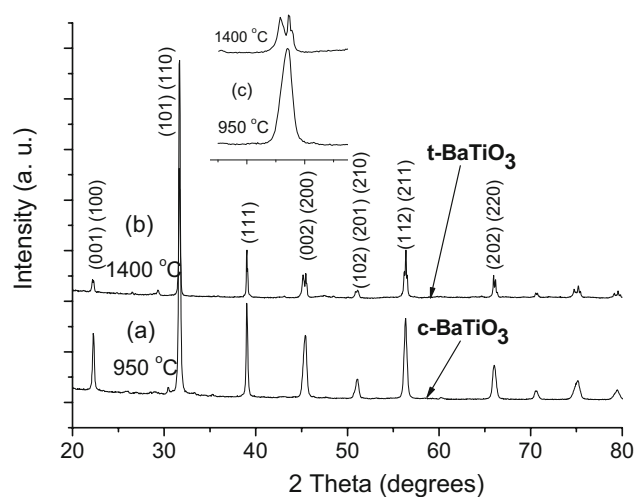


**Fig. 4** X-ray diffraction patterns of the  $BTS_{13}$  pellets obtained by SPS and annealed at 950 °C in oxygen (a) and then, conventional sintered at 1400 °C (b). Inset (c) shows detail of (002) and (200) peaks resulted by splitting of (200) peak at 1400 °C

## Dielectric properties

The variations of relative permittivity and of  $\tan \delta$  with temperature, at various frequencies (10 Hz, 100 Hz, 1 kHz, 10 kHz and 100 kHz), for the SPS pellets after the final conventional sintering at 1400 °C are shown in Fig. 5a, b.

The highest dielectric constant of  $\text{BTS}_{13}$  was 6550 at 10 Hz and decreased up to 5,500 at 100 kHz, at the Curie point temperature (Fig. 5a). The temperature of Curie point ( $T_c$ ) was  $T_c = 63$  °C. This value of Curie temperature point, higher than that indicated in literature [6, 7, 15], can be attributed to partial reduce of  $\text{Ti}^{4+}$  to  $\text{Ti}^{3+}$  and to chemistry imbalances created by SPS at grain boundaries. The dielectric loss, at Curie temperature, was 0.013 at 10 Hz and increased up to 0.1 at 100 kHz (Fig. 5b). A small influence of the frequency on the dielectric properties was observed.

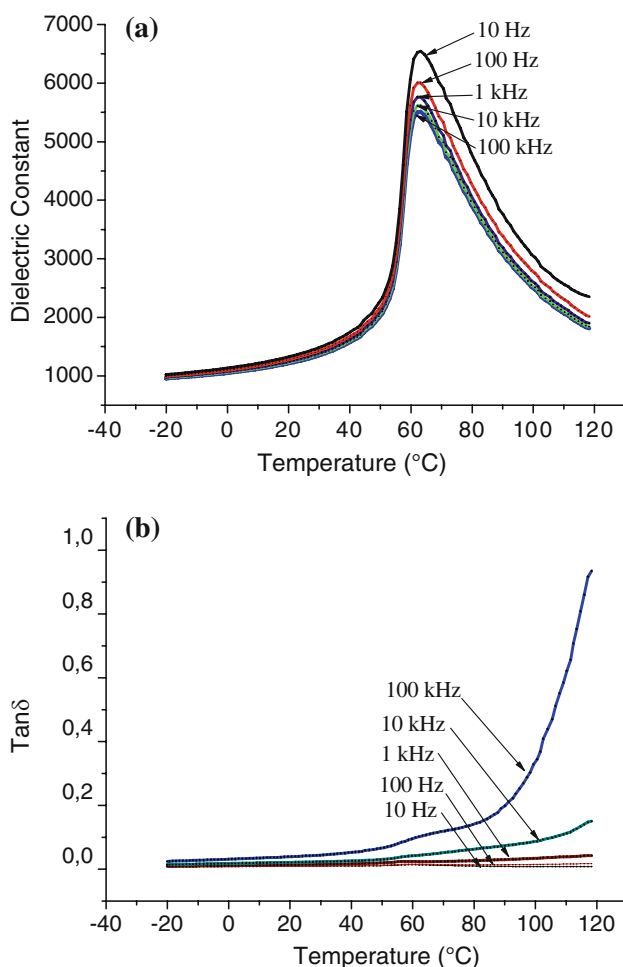


**Fig. 5** Temperature and frequency dependence of **a** dielectric constant and **b** loss tangent ( $\delta$ ) for  $\text{BTS}_{13}$  ceramic sintered by SPS and conventional method

## Conclusions

We used SPS method for a fast initial first step of pressing-sintering process of barium titanate stannate powders. The as-obtained SPS pellets consist of submicron (300–500 nm) grains. Because the room temperature permittivity, at 1 kHz, for  $\text{BaTiO}_3$  ceramics shows an apparent maximum at grain size in the range of about 1  $\mu\text{m}$  [19, 20], we continued the sintering process by the conventional method to increase grain size. In this work, final ceramic had a grain size of about 2  $\mu\text{m}$  with high grain size uniformity. The second step of conventional sintering also resulted in the conversion of the cubic phase observed after SPS processing-step into tetragonal single phase. Final ceramic had a density of about 92% of the theoretical value and good dielectric properties ( $\epsilon_r = 6,550$ ,  $\tan \delta = 0.078$ ) at Curie temperature,  $T_c = 63$  °C and 10 Hz. The values of the dielectric characteristics of  $\text{BTS}_{13}$  ceramics consolidated by SPS and conventional sintering methods are in good agreement with literature data.

Despite the drawback of carbon contamination at the surface of the  $\text{BTS}_{13}$  ceramic during SPS process, the benefits of the proposed combined two-step sintering method to prepare  $\text{BTS}_{13}$  solid solution consist in: the control of grain size and morphology, the control of oxygen deficiency and the control of the cubic  $\text{BTS}_{13}$  conversion into tetragonal  $\text{BTS}_{13}$  phase with high permittivity.

**Acknowledgement** We would like to gratefully acknowledge P. Badica for very useful and profitable discussions.

## References

- Subbarao EC (1981) *Ferroelectrics* 35:143
- Vivekanandan R, Kutty TRN (1988) *Ceram Int* 14:207
- Wernicke R (1978) *Ber Dtsch Keram Ges* 55:356
- Brauer H (1970) *Z Angew Phys* 29:282
- Smolensky GA (1970) *J Phys Soc Jpn* 28:26
- Yasuda N, Ohwa H, Asano S (1996) *Jpn J Appl Phys* 35:5099
- Oh K, Uchino K, Cross LE (1994) *J Am Ceram Soc* 77:2809
- Xiaoyong W, Yujun F, Xi Y (2003) *Appl Phys Lett* 83:2031
- Mueller V, Beige H, Abicht H-P (2004) *Appl Phys Lett* 84:1341
- Munir ZA, Tamburini UA, Ohyanagi M (2006) *J Mater Sci* 41:763. doi:10.1007/s10853-006-6555-2
- Nava ZV, Fritsch SG, Tenailleau C, Lebey T, Durand B, Ching JYC (2009) *J Electroceram* 22:238
- Takeuchi T, Suyama Y, Sinclair DC, Kageyama H (2001) *J Mater Sci* 36:2329. doi:10.1023/A:1017585209648
- Li B, Wang X, Cai M, Hao L, Li L (2003) *Mater Chem Phys* 1:173
- Cernea M, Piazza D, Manea A, Vasile E, Galassi C (2007) *J Am Ceram Soc* 90:1728
- Geske L, Lorenz V, Muller T, Jager L, Beige H, Abicht HP, Müller V (2005) *J Eur Ceram Soc* 25:2537
- Richerson DW (1992) *Modern ceramic engineering: properties, processing, and use in design*, 2nd edn, rev. and expanded. Marcel Dekker, Inc, New York, p 128

17. Buttner RH, Maslen EN (1992) *Acta Crystallogr B* 48:764
18. Kwei GH, Lawson AC, Billinge SJL, Cheong SW (1993) *J Phys Chem* 97:2368
19. Li B, Wang X, Li L, Zhou H, Liu X, Han X, Zhang Y, Qi X, Deng X (2004) *Mater Chem Phys* 83:23
20. Arlt G, Hennings D, deWith G (1985) *J Appl Phys* 58:1619